Implementation of Feed-in Tariffs into Multi-Energy Systems

M. Schulze and P. Crespo Del Granado

Abstract**—**This paper considers the influence of promotion instruments for renewable energy sources (RES) on a multi-energy modeling framework. In Europe, so called Feed-in Tariffs are successfully used as incentive structures to increase the amount of energy produced by RES. Because of the stochastic nature of large scale integration of distributed generation, many problems have occurred regarding the quality and stability of supply. Hence, a macroscopic model was developed in order to optimize the power supply of the local energy infrastructure, which includes electricity, natural gas, fuel oil and district heating as energy carriers. Unique features of the model are the integration of RES and the adoption of Feed-in Tariffs into one optimization stage. Sensitivity studies are carried out to examine the system behavior under changing profits for the feed-in of RES. With a setup of three energy exchanging regions and a multi-period optimization, the impact of costs and profits are determined.

Keywords**—**Distributed generation, optimization methods, power system modeling, renewable energy.

I. Introduction

The European Commission, as the executive branch of the EU, is today the central authority in Europe for the production of renewable energy. Ten years ago, the case was different. Individual countries were at the cutting edge of new technologies, while a comprehensive European energy policy remained out of scope. Some countries were driven by ecological and sustainability trends; others like Germany had no other options left, after the nuclear power phase-out. In November 2000, the European Commission submitted its Green Book focusing on a diversified, decentralized, cost-effective, stable and clean energy supply for Europe [1].

The short-term growth in the Renewable Energy Sources (RES), as reported in Table I, was a promising evolution, and it has not yet come to an end. With respect to the stochastic nature of many new renewables, like wind or solar power, problems occurred in central Europe. The massive blackout in Autumn 2006 caused an interruption of supply for about 15 million households [2]. It now seems crucial for the development of the future power supply in Europe to combine long-term modeling of integrated and decentralized energy systems with an optimized system control focusing on renewables and storages. This paper is based on a novel concept for modeling and optimization of multiple energy carrier systems in synergy for long time horizons, such as 50 years into the future. Current trends in financing new renewable energy production were analyzed and the existing modeling concept adapted [3-5].

M. Schulze is with the Swiss Federal Institute of Technology Zurich, Zurich, Physikstrasse 3, 8092 Switzerland (phone: +41-44-632-83-73; fax: +41-44-632-12-02; e-mail: mschulze@ethz.ch).

P. Crespo Del Granado is with the George Washington University, 1776 G Street NW Suite108, Washington DC, 20052 USA (e-mail: pedro@gwu.edu).

II. Feed-in Tariffs in Europe

In Table I, a survey of the development of RES reflects the share of RES of the gross electricity consumption. Belgium primarily utilizes nuclear energy production, so a shift towards less CO_2 emissions and more RES is difficult. Germany has a lot of hard coal and lignite fired plants, which allow a reduction of emissions. Together with the promoted wind energy, the nuclear power phase-out is possible. Other countries like Austria already have a high share of RES, typically from hydropower.

TABLE I
Renewable Energy in the European Union

EU Country	Instrument Introduction in the year	Promotion Scheme	Baseline 1997	Targets for 2010	Reached in 2006	Goal reached? 2006 share compared to 2010 targets in %
			Renewables in % of the gross electricity consumption			
Austria	2003	F, I	67.5	78.0	56.6	-103.8
Belgium	2003	Q, F	1.0	6.0	3.9	58.0
Cyprus	2004	F	0.0	6.0	0.0	0.0
Czech Rep.	2002	F, I	3.5	8.0	4.9	31.1
Denmark	2002	Q, F	8.8	29.0	25.9	84.7
Estonia	1998	F	0.1	5.1	1.4	26.0
Finland	2001	I, F	25.3	31.5	24.0	-21.0
France	2001	F	15.2	21.0	12.4	-48.3
Germany	1991	F	4.3	12.5	12.0	93.9
Greece	2003	F	8.6	20.1	12.1	30.4
Hungary	2003	F	0.8	3.6	3.7	103.6
Ireland	2005	F	3.8	13.2	8.5	50.0
Italy		Q, F	16.0	25.0	14.5	-16.7
Latvia	2003	F	46.7	49.3	37.7	-346.2
Lithuania	2003	F	2.6	7.0	3.6	22.7
Luxembourg	2003	F, I	2.0	5.7	3.4	37.8
Netherlands	2003	F, I	3.5	9.0	7.9	80.0
Poland		Q	1.8	7.5	2.9	19.3
Portugal	1988	F	38.3	39.0	29.4	-1271.4
Slovakia		I	14.5	31.0	16.6	12.7
Slovenia	2002	F	26.9	33.6	24.4	-37.3
Spain	1994	F	19.7	29.4	17.3	-24.7
Sweden		Q, I	49.1	60.0	48.2	-8.3
UK		Q, I	1.9	10.0	4.6	33.3

Furthermore, different promotion schemes were used: Quota systems (Q) with Green tags and Feed-in Tariffs (F), in addition to fiscal incentives (I). Overall, the performance of the Quotas was poor, in comparison to the Feed-in Tariffs, as in Table 1 and in [6-9]. Switzerland, not an EU member, has a quite different background. Hydropower (25.3% run-of-river power plants and 30.0% storage power plants) and nuclear power (40.0%) together provide 95.3% of the electricity production, CO_2-low and cheap. Feed-in Tariffs make cost-covering RES possible, but governmental incentives for the promotion of more RES are poorly implemented. In order to reduce the primary energy demand and the CO_2 emissions, the focus was set on zero- resp. low-energy houses. Large scale RES are often in conflict with local residents, like the geothermal project in the city of Basel [10].

The European Strategic Energy Technology Plan (SET-Plan) is an overview of the energy- and transport-related R&D inside Europe, including a comparison with the USA and Japan [11,12]. The study points to varieties in public spending on overall R&D. Japan dedicates more than 3% of its GDP on R&D, whereas the USA (~2.6%) and the EU (1.9%) spend less. Also remarkable are the differences inside the EU especially for energy R&D: France provides 12 times more money than the UK, 720 mEUR and 60 mEUR resp. in 2005. Nevertheless, absolute values of private and public funding should be compared with the reached goals in Table I; additionally, the recently published global analysis of M. Mendonça [13] illustrates costs and returns.

III. Modeling of Renewables

At the ETH Zurich, a macroscopic model for the description of multi-carrier energy flow and optimization has been developed [14,15]. The theoretical concept uses a greenfield approach and was named the "Energy Hub". An Energy Hub is a local cluster of energy converter and storage elements, an input of energy into the Hub, and an output to a load. Energy therefore refers not only to electricity. Stabilizing energy consumption, integrating renewable energy sources and reducing CO_2-emissions can be optimized in a single modeling framework, if different primary, secondary and tertiary energy carriers are combined inside the simulation. Consequently, the Energy Hub concept can include all possible energy carrier, mainly electricity, natural gas, fuel oil and district heating. In Fig. 1 the joined input and output energy flows are outlined, where bold capitals name vectors or matrices with the power flow of different energy carriers. The input contains two vectors: one vector **P** represents the energy taken from the grid and the other vector **R** represents the local renewable energy production, e.g. from photovoltaic's or a wind turbine. The load is connected as the **L** vector together with the feed-in vector **T** at the output side of the Hub. Input and output are linked via the coupling matrix **C**, which describes the converter elements. Theoretical storage devices inside the Hub exchange their energy with additional vectors **Q** and **M**. This will be investigated in the near future.

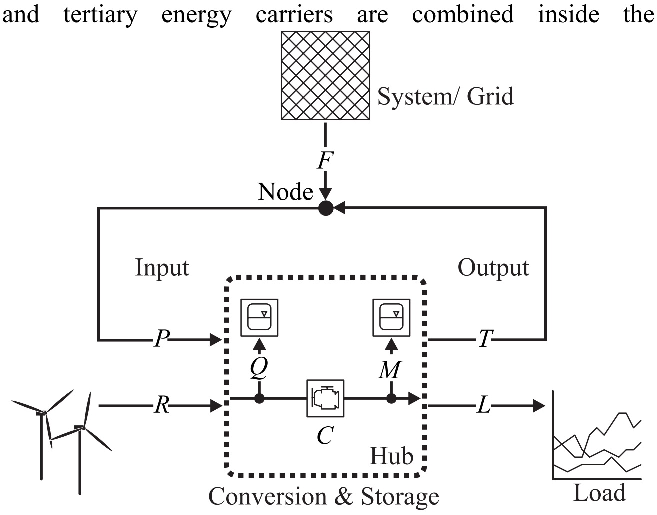

Fig. 1: The Energy Hub model

System $\mathfrak{S}$	Network $\mathfrak{E}\left(\mathbf{F}_{\mathfrak{N}_i \to \mathfrak{N}_j}\right) = \left(el \quad co\right)^T$	External $\mathfrak{E}\left(\mathbf{F}_{\mathfrak{N}_i \to \mathfrak{N}_x}\right) = \left(ng\right)$
Node $\mathfrak{N}$	$\mathfrak{E}\left(\mathbf{F}_{\mathfrak{N}_i \to \mathfrak{H}_i}\right) = \left(el \quad ng \quad co\right)^T$	
Hub $\mathfrak{H}$	$\mathfrak{E}(\mathbf{P}) = (el \quad ng)^T$ $\mathfrak{E}(\mathbf{R}) = (bm)$ Input	$\mathfrak{E}(\mathbf{T}) = (co)$ $\mathfrak{E}(\mathbf{L}) = (el \quad he)^T$ Output

Fig. 2: Example of different energy carriers within the model (el-electricity, co-coolant, ng-natural gas, bm-biomass, he-heat)

According to Fig. 1, each Hub is connected via a node to the supply grid. The system or grid consists of nodes and represents the investigation area. If the network of nodes is not operated in isolation, one or several connections to the outside are described as external; see Fig. 2 with an example of different energy carriers on system, node and hub level. The fracture capital $\mathfrak{E}$ indicates the energy carrier, $\mathfrak{S}$ indicates the systems, and the nodes $\mathfrak{N}$ and $\mathfrak{H}$ are the Hubs. This discrimination was established in order to allow nodes without Hubs, which might be used similar to physical waypoints of existing overhead lines or cables. In

Fig. 2 it is obvious that not every energy carrier exists in every level. Electricity has a connection from the load through the network within the system to the outside, like in today's grids. Coolant is produced inside the Hub and distributed only inside the system, not to the outside. Biomass is a Hub-local energy carrier, and natural gas is transported without network from outside the node, e.g. by a tank truck. Summing up, Hubs with multiple energy carriers can be written as a single equation for each Hub:

$$\left(\mathbf{L}_\beta + \mathbf{T}_\beta\right) = \mathbf{C}_{\alpha\beta} \cdot \left(\mathbf{P}_\alpha + \mathbf{R}_\alpha\right) \forall \alpha, \beta \in \mathfrak{E}. \quad (1)$$

The input and output energy carrier can be different. The coupling of input and output to the grid is similar.

$$\mathbf{F}_{\alpha \wedge \beta} = \mathbf{P}_\alpha - \mathbf{T}_\beta \forall \mathfrak{H} \forall \alpha, \beta \in \mathfrak{E} \quad (2)$$

Early work [14] carried out at the "Vision of Future Energy Networks" group at the ETH Zurich contributed **P**, **L** and **C** to the Hub model. The necessity of the additional vectors **R** and **T** has been proven in [3], where a special focus on renewable energy production was set. For optimization tasks, the matrix of converter elements is usually fixed, the production of renewable energy is given, and the load demand is known for a certain time. Free parameters are the amount of energy taken from and sent to the grid via the node. Costs related to the objective function and the vector **P** could be prices for the energy, CO_2 emissions, or an arbitrary cost value. Instead of using single cost values, Pareto optimality is possible. Considering benefit trade off for the feed-in of energy, represented with the **T** vector, the objective function $\mathfrak{F}(x)$ includes both, costs and benefits for each Hub $\mathfrak{H}$:

$$\begin{aligned} &\text{Minimize} && \mathfrak{F}\left(\mathbf{P},\mathbf{T},THC\right) \\ &\text{subject to} && \left(\mathbf{L}+\mathbf{T}\right)-\mathbf{C}\cdot\left(\mathbf{P}+\mathbf{R}\right)=0 \\ & && h\left(\mathbf{P},\mathbf{T}\right)\le 0 \end{aligned} \tag{3}$$

The objective function contains both variable vectors (**P**, **T**) and the total Hub costs *THC*. For the total Hub costs, system marginal costs $\mathbf{\Psi}$ and benefits $\mathbf{\Phi}$ in monetary-unit per-unit are used in (4). Summing over all Hubs in (5) and over all time steps in (6) yield the total system costs *TSC*. Like the total Hub costs, the total system costs are given in monetary-unit.

$$\mathbf{\Psi}=\frac{\partial THC}{\partial \mathbf{P}} \qquad \mathbf{\Phi}=\frac{\partial THC}{\partial \mathbf{T}} \tag{4}$$

$$\sum_{i\in\mathfrak{H}} THC_i=\sum_{i\in\mathfrak{H}} \mathbf{\Psi}^T\cdot\mathbf{P}_i-\mathbf{\Phi}^T\cdot\mathbf{T}_i \tag{5}$$

$$TSC=\sum_t TSC\left(t\right)=\sum_t\sum_{i\in\mathfrak{H}} THC_i\left(t\right) \tag{6}$$

Applying the Feed-in Tariffs to the Energy Hub model, one could refer the benefits $\mathbf{\Phi}$ either to the vector **R** or to the vector **T**. From a household's viewpoint, where separate electric meters are installed for the produced power (e.g. solar) and the consumed power (from grid), a relation between $\mathbf{\Phi}$ and **R** seems best. Marginal costs $\mathbf{\Psi}$ and benefits $\mathbf{\Phi}$ together with the vectors **P** and **T** yields the total costs *TC* and total benefits *TB* in (7). The definition of distributed generation itself signifies something different: small scale local production for local demand. Therefore the viewpoint of an utility was chosen. Only the surplus of energy produced and fed into the grid will be paid.

$$THC_i=TC_i-TB_i\forall i\in\mathfrak{H} \tag{7}$$

In order to avoid self-energizing loops between **P** and **T** in (2), certain rules must be applied. If a benefit is higher than the related costs, an optimization would sell energy in **T** directly from the input **P** in an endless loop; the connection **F** to the grid is not limiting. Only the share coming from **R** inside **T** should be paid.

IV. Optimization Example

A. Broad description

This described model of a multi carrier energy flow was applied to a pragmatic situation involving three different energy hubs. Hub configurations, components and features have been established from a current case study involving a combination of domestic, commercial and industrial areas. The structure of the system is represented in Fig. . This arrangement is based on supplying the region's energy requirements so it can be close to the consumer's. These decentralized energy units supply the load demand levels **L** by means of a local renewable input **R** and the **P** power vector coming from an external grid or from the energy distributed $\mathbf{T}_{\mathbf{dh}}$ from Hub-1.

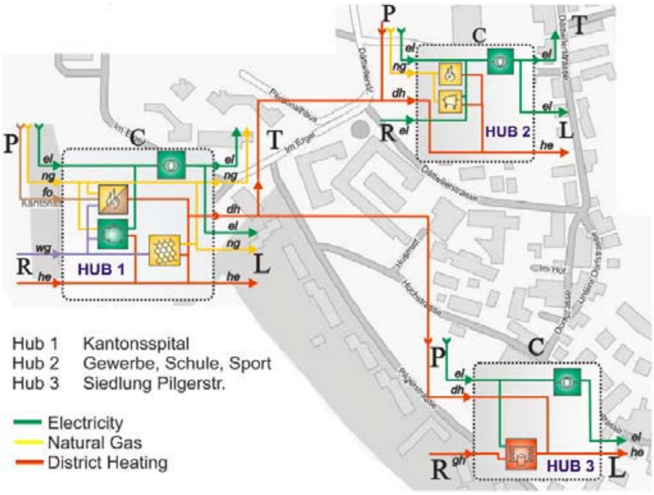

Fig. 3: Scenario design of the Energy Hub model

Each hub's coupling matrix **C** components are determined by the hub energy mechanism of conversion and transmission. Hub-1, for instance, is fed by a wood gasification facility $\mathbf{R}_{\mathbf{wg}}$ that is connected to a combined heat and power unit (CHP green box) , a purification of wood gas to natural gas(lower-right yellow icon) and a burner with natural gas and heating oil (yellow brown symbol). Furthermore, there is a transformer fed by the power unit and the electricity coming from the grid. The same type of transformer is omnipresent in all hubs. In the case of Hub-2, there is micro-turbine MT (yellow box with a trapezoid) containing a thermal and electrical factor, and right above it a furnace; both are fed by natural gas coming from the grid. Here the renewable $\mathbf{R}_{\mathbf{el}}$ provides a constant electricity supply throughout the day from solar photovoltaic. Lastly Hub-3 has a geothermal probe GP to produce heat which is supplied by electricity or by absorbing heat derived from underground.

B. *Modeling and Optimization Period*

Designed for this hub network, the optimization approach used solves a multi-period optimal dispatch with a multi carrier optimal power flow. The period length of the simulation is one-month spread in 2689 time-steps; the real time difference between times step is 15 minutes, where the demand **L** is updated. Every optimization time-step is carried out in the MATLAB-function *fmincon* with a predefined objective function and its linear and non-linear constrains. The optimization period chosen for this example was between:

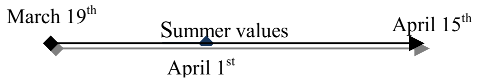

For all hubs, the optimized variables are the vectors **P** and **T** as well as the dispatch vectors $\boldsymbol{\nu}$ which are established on each possible energy carrier's node coming up from the input side of the hub **P** & **R**. The **P** -vector corresponds to the inputs of external sources as electricity, natural gas and fuel oil. The **R** -vector reflects the internal renewable energies sources, such as solar and wind for electricity, wood gas and geothermal for heating, or gas. Consequently, as previously described **R** and **L** turned out to be predetermined values.

Given the Hubs' characteristics, their coupling matrixes define a structured set of constraints containing the preset values and the variables optimized in the model. Hence, the system matrix C present in the hubs is as follows: Hub-1 components are:

$$\mathbf{C}=\begin{pmatrix}\eta_{el-el} & c_{12} & 0 & 0\\ 0 & c_{22} & 0 & 0\\ 0 & c_{32} & \eta_{fo-dh/he} & 1\end{pmatrix}$$

With the parameters:

$$\begin{aligned}c_{12} &= \nu_{\mathrm{I}}^{ng}\cdot\eta_{ng-el}\cdot k+\nu_{\mathrm{I}}^{wg}\cdot\eta_{wg-el}\cdot(1-k)\\ c_{22} &= \nu_{\mathrm{II}}^{ng}\cdot 1\cdot k+\nu_{\mathrm{II}}^{wg}\cdot\eta_{wg-ng}\cdot(1-k)\\ c_{32} &= \left(\nu_{\mathrm{III}}^{ng}\cdot\eta_{ng-dh/he}+\nu_{\mathrm{I}}^{ng}\cdot\eta_{ng-dh/he}^{CHP}\right)\cdot k\\ &\quad+\left(\nu_{\mathrm{III}}^{wg}\cdot\eta_{wg-dh/he}+\nu_{\mathrm{I}}^{wg}\cdot\eta_{wg-dh/he}^{CHP}+\nu_{\mathrm{II}}^{wg}\cdot\eta_{wg-dh/he}^{PUR}\right)\\ &\quad\cdot(1-k)\end{aligned} \tag{8}$$

Hub 2 designed C matrix and elements:

$$\mathbf{C}=\begin{pmatrix}\eta_{el-el} & c_{12} & 0 & 0\\ 0 & 0 & 0 & 0\\ 0 & c_{32} & 0 & 1\end{pmatrix}\qquad \begin{aligned}c_{12} &= \nu^{ng}\cdot\eta_{MT/ng-el}\\ c_{32} &= \left(1-\nu^{ng}\right)*\eta_{F/ng-he}+\nu^{ng}*\eta_{MT/ng-he}\end{aligned} \tag{9}$$

Hub 3 designed C matrix and elements:

$$\mathbf{C}=\begin{pmatrix}c_{11} & 0 & 0 & 0\\ 0 & 0 & 0 & 0\\ c_{13} & 0 & 0 & 1\end{pmatrix}\qquad \begin{aligned}c_{11} &= \nu^{el}\cdot\eta_{el-el}\\ c_{13} &= \left(1-\nu^{el}\right)\cdot\eta_{GP/el-he}\end{aligned} \tag{10}$$

Every $\boldsymbol{\eta}$ is a constant efficiency factor that is properly defined in Table II (appendix). k in Hub1 is defined as the natural gas share of the total gas amount (wood gas and natural gas).

These arrays of equations in conjunction with the objective function are aimed to minimize the total system costs TSC (6). Nevertheless, to have a better understanding of the model, a sensitivity analysis is performed by changing the coefficient parameters in the objective function. In this case a variation for $\boldsymbol{\Phi_{el}}$ from 0 to 20 mu/pu (monetary unit per unit) and $\boldsymbol{\Phi_{dh}}$ from 0 to 40 mu/pu was accomplished.

C. Results - Sensitivity Analysis

Once the simulation period had been completed for the entire set of price combinations of $\boldsymbol{\Phi_{el}}$ and $\boldsymbol{\Phi_{dh}}$, the results pointed out that these variations influenced only Hub-1. Evidently, as observed in Fig. , for Hub-3 the **T** vectors are nonexistent. Thus, Hub-3 optimal values for a given time are constant for every variation. This situation also describes why in Hub-2 there is not an appreciable change. Although in this case there is a feed in vector $\mathbf{T_{el}}$, the peak variation in this vector is 20 mu, which is lower than the power input vector $\mathbf{P}_{el}$. Hence, only variation higher than 25 mu ($\mathbf{P}_{el}$ cost lowest value Fig.) can produce a change in the value of the optimal solution for $\mathbf{T_{el}}$. As a result, the electricity carrier is unaffected by the intended price variation in all hubs.

The minimized objective function's values are illustrated in the three dimensional plot in Fig. 4, which is a representation of the total system cost in blue obtained by the simulation at a particular step with its price variation. As it can be evaluated, there are multiple lines that create a dense and thick pattern for *TC*, *TB* and *TSC*. The reason for having such agglomeration of lines is because there are 2689 lines with each one containing 11 different solutions intended for this sensitivity analysis ($\boldsymbol{\Phi_{el}}$ - 0 to 20; $\boldsymbol{\Phi_{dh}}$ -0 to 40). In this figure, the *TSC* is detached in its two components (the total cost related to **P** in red and the total benefit related to **T** in green).

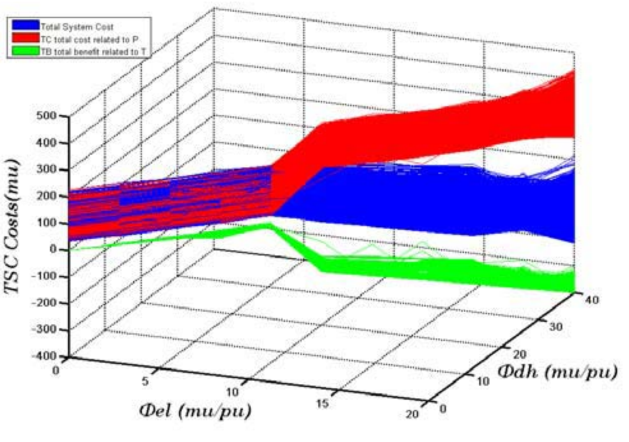

Fig. 4: Solutions of the entire period vs. variations of Phi

In this figure, while the **T** feed-in vectors' variation increases, the **P** input vector increases due to the weight generated by **T**, since the equation (1) needs to be balanced. Therefore the cost function solutions (blue) show the tendency of the subtraction of TC minus TB. Nevertheless, this pattern is not present at the first variations in the model, where there is constant behavior. Fig. 4 shows a mixed section of blue and red lines that are parallel to the green lines. Once the lines reach the variation point $\mathbf{T_{el}}$=10 and $\mathbf{T_{dh}}$=20, here a significant change occurs in the feasible region of the cost function. Such a leap can be explained by looking at Fig. in the appendix, where the cost of the fuel oil is constant at 15 mu. Clearly the optimal power flow would obtain a reduction in the cost when it reaches a value higher than 15 mu, given that the selling price at the $\mathbf{T_{dh}}$ price helps to minimize the cost. As a result, the burner in Hub-1 purchases as much fuel oil $\mathbf{P_{fo}}$ as possible to obtain a benefit from district heating. A maximum value per units (pu) restriction for any carrier is 10 units.

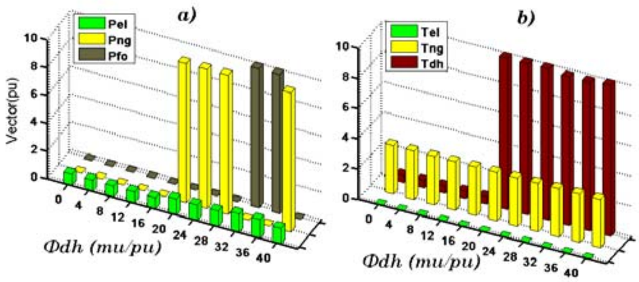

Fig. 5: Optimal solution at time step 2000 after the summer values
a) Hub-1 input power vectors, b) Hub-1 Feed in vectors

As shown in Fig. 7 (appendix), important fluctuations take place when the cost adjusts to the summer values. The natural gas tariff changes in April 1st from 17.5 to 13.75 mu. In addition, the cost for district heating experiences a variation from 60.25 to 51.25 mu. However, district heating modification is not central to the results since the upper limit $\mathbf{\Phi}_{dh}$ variation is 40 mu as well as electricity price, which fluctuates from 25 to 55 mu. Therefore, the only energy carriers that are expected to show a pattern of variation analogous to $\mathbf{\Phi}_{dh}$ prices are $\mathbf{P_{fo}}$, $\mathbf{P_{ng}}$ and $\mathbf{T_{dh}}$.

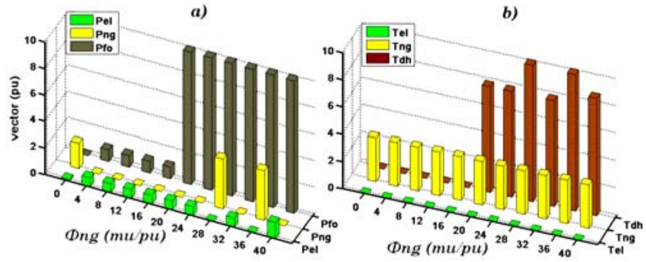

Fig. 6: Optimal solution at time step 516 before the summer values
a) Hub-1 input power vectors, b) Hub-1 Feed in vectors

As a result, to have better insight in the model, Fig. and Fig. represent a contrast of what happens with a given solution before and after these summer values take place. In both figures, the jump that occurs when $\mathbf{\Phi}_{dh}$ arrives at 20 mu can once again be observed. Moreover, as it was discussed earlier, $\mathbf{P_{el}}$ and $\mathbf{T_{el}}$ do not experience any irregular change even with this new modification. It is also palpable that $\mathbf{T_{ng}}$ will remain constant because it has a continuous natural gas supply coming from the purifier. Although an occasional increase could be possible, it would not occur often since the $\mathbf{\Phi_{ng}}$ coefficient is zero, which means that the system is giving away (at no cost) natural gas to the grid.

A main difference between these two figures comes from $\mathbf{P_{ng}}$. The optimization algorithm evidently intends to take away a benefit from $\mathbf{P_{ng}}$ as well as from $\mathbf{P_{fo}}$ since these are the most economical carriers. For that reason there is a switch or a merger between these two in order to produce $\mathbf{T_{dh}}$ at the burner element.

V. Conclusion

Based on this model of renewable energy sources, Feed- in Tariffs potentialities are greatly emphasized due to the benefits of rewarding actual local energy production. This macroscopic model, which diversifies the energy supply, shows that by optimizing the different energy carriers, the cost of renewable energy sources can be reduced. This cost is reduced according to the range of weights imposed with the variation of $\mathbf{\Phi_{dh}}$ in the function cost. The solutions prove that there is a cost-effective way to impact the overall benefit and satisfy the local demand $\mathbf{L}$. By contrast, high prices for $\mathbf{\Psi_{el}}$ proved to be complicated to attain having not profit whatsoever. In real circumstances this could discourage technical innovation in renewable electricity generation.

With regards to further analysis, a deeper assessment of other energy carriers would help to find more weaknesses and strengths of the model. This assessment should also consider finding and determining more Hubs' elements and their readiness for different cost-benefit scenarios such as the one presented here.

Appendix

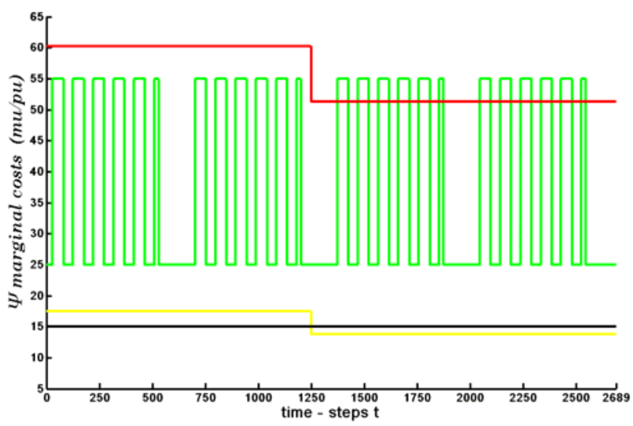

Fig. 7: Costs for the input power during the simulation period

TABLE II
HUB-1 EFFICIENCIES / OPTIMIZATION EXAMPLE

Symbol	Value	Conversion	Element
η_{el-el}	0.994	Electricity to electricity	Transformer
$\eta_{ng-dh/he}$	0.90	Natural gas to district heating or heat	Burner
$\eta_{fo-dh/he}$	0.85	Fuel oil to district heating or heat	Burner
$\eta_{wg-dh/he}$	0.80	Wood gas to district heating or heat	Burner
η_{ng-el}	0.30	Natural gas to electricity	CHP
η_{wg-el}	0.27	Wood gas to electricity	CHP
$\eta_{ng-dh/he}^{CHP}$	0.40	Natural gas to district heating or heat	CHP
$\eta_{wg-dh/he}^{CHP}$	0.38	Wood gas to district heating or heat	CHP
η_{wg-ng}	0.80	Wood gas to natural gas	Purifier
$\eta_{wg-dh/he}^{PUR}$	0.08	Wood gas to district heating or heat	Purifier
HUB-2 EFFICIENCIES / OPTIMIZATION EXAMPLE			
η_{el-el}	0.994	Electricity to electricity	Transformer
$\eta_{F/ng-he}$	0.90	Natural gas to heat	Furnace
$\eta_{MT/ng-he}$	0.4	Natural gas to heat	Micro Turbine
$\eta_{MT/ng-el}$	0.3	Natural Gas to Electricity	Micro Turbine
HUB-3 EFFICIENCIES / OPTIMIZATION EXAMPLE			
η_{el-el}	0.994	Electricity to electricity	Transformer
$\eta_{GP/el-he}$	4.56	Electricity to heat	Geothermal Probe

ACKNOWLEDGMENT

The authors would like to thank the Regionalwerke AG Baden and the Agency of Energy - City of Baden for the prosperous cooperation. Also a special thank goes to ABB, Areva, Siemens and the Swiss Federal Office of Energy for their contribution to the VoFEN-project and finally to all group members and Prof. K. Fröhlich.

REFERENCES

[1] Green Paper, *Towards* a European *Strategy for the Security of Energy Supply*, Commission of the European Communities, Brussels, Belgium, 29/11/2000.

[2] Final Report, *System Disturbance on 4 November 2006*, Union for the Co-ordination of Transmission of Electricity (UCTE), Brussels, Belgium, 30/01/2007.

[3] M. Schulze, L. Friedrich and M. Gautschi, "Modeling and Optimization of Renewables: Applying the Energy Hub Approach", *IEEE International Conference on Sustainable Energy Technologies*, Singapore, November 2008.

[4] P. Favre-Perrod and M. Schulze, "Synergies among several energy carrier systems in future energy networks", *15th International Symposium on High Voltage Engineering*, Ljubljana, Slowenia, August 2007.

[5] M. Schulze and A. Hillers, "Energy Hubs für die urbane Energiever-sorgung", *10th Symposium Energieinnovation*, Graz, Austria, February 2008.

[6] A. Campoccia, L. Dusonchet, E. Telaretti, and G. Zizzo, "Financial Measures for Supporting Wind Power Systems in Europe: A Comparison between Green Tags and Feed'in Tariffs", *19th International Symposium on Power Electronics, Electrical Drives, Automation and Motion*, Ischia, Italy, June 2008.

[7] A. Campoccia, L. Dusonchet, E. Telaretti, and G. Zizzo, "Feed-in Tariffs for Grid-connected PV Systems: The Situation in the European Community", *Power Tech '07*, Lausanne, Switzerland, July 2007.

[8] T. Traber, "Impact of Market Power on Price Effects of the German Feed-in Tariff under the European Emission Trading System", *5th International Conference on the European Electricity Market*, Lisbon, Portugal, May 2008.

[9] Report, *Europe's energy position – present & future*, Directorate-General for Energy and Transport, European Commission, Luxembourg, 2008.

[10] M. Häring, U. Schanz, F. Ladner, and B. Dyer, „Characterisation of the Basel 1 enhanced geothermal system", *Geothermics Vol. 72, Issue*, pp. 469-495, October 2008.

[11] Technology Map, *A European Strategic Energy Technology Plan (SET-Plan)*, Commission of the European Communities, Brussels, Belgium, 22/11/2007.

[12] Capacities Map, *A European Strategic Energy Technology Plan (SET-Plan)*, Commission of the European Communities, Brussels, Belgium, 22/11/2007.

[13] M. Mendonça, Feed-in Tariffs: *Accelerating the Deployment of Renewable Energy*. London: Earthscan, 2009, ch. 4-7.

[14] M. Geidl and G. Andersson, "Optimal Power Flow of Multiple Energy Carriers", *IEEE Transactions on Power Systems, Vol 22, No 1*, 2007.

[15] P. Favre-Perrod, A. Hyde, and P. Menke, "A Frame-work for the study of multi-energy networks", *2nd SmartGrids Technology Plattform General Assembly*, Bad Staffelstein, Germany, November 2007.